Adjusting For Batch Effects In Two Photon Imaging Recordings Of The Retinal Inner Plexiform Layer

David A. Klindt[1,2,3]*, Luke E. Rogerson[1,2,3]*, Zhijian Zhao[1,3], Klaudia Szatko[2,3], Katrin Franke[2,3], Dmitry Kobak[3], Alexander S. Ecker[1,2,4,5], Matthias Bethge[1,2,4,5], Philipp Berens[1,2,3,6]*, Thomas Euler[1,2,3]*

* equal contributions [1] Centre for Integrative Neuroscience, University of Tübingen, Germany [2] Bernstein Center for Computational Neuroscience, Tübingen, Germany [3] Institute for Ophthalmic Research, University of Tübingen, Germany
[4] Institute for Theoretical Physics, University of Tübingen [5] Center for Neuroscience and Artificial Intelligence, Baylor College of Medicine, Houston, TX, USA [6] Department of Computer Science, University of Tübingen, Germany

EBERHARD KARLS UNIVERSITÄT TÜBINGEN

contact: klindt.david@gmail.com

Abstract

The retina decomposes visual stimuli into parallel channels which encode different features of the visual environment, including light increments, and decrements, edge orientation and direction and colour. Central to this parallelisation is the excitatory feedforward network composed sequentially of photoreceptors, bipolar cells and ganglion cells. Two-photon (2P) imaging with an electrically tuneable lens allows us to scan vertical cross-sections of excised intact retina, and to observe glutamate release at bipolar cell terminals across the inner plexiform layer (IPL), where different bipolar cell types stratify at different depths. To integrate recordings across retinae, and jointly disentangle the feature channels from the observed data, it is necessary to remove any batch effects, i.e. inter-experimental variation caused by e.g. temperature, jitter, bleaching, indicator concentration and/or laser intensity.

Imaging the complete IPL

Here, we introduce a fast axial x-z scanning, a method to image across the whole IPL in the intact, whole-mount retina. It allows us to record from all bipolar cell channels virtually simultaneously. We equipped a 2P microscope (Fig. 1; see [1]) with an ETL, which enables fast focus shifting along the z axis (F. Helmchen, personal communication; see also [3]).

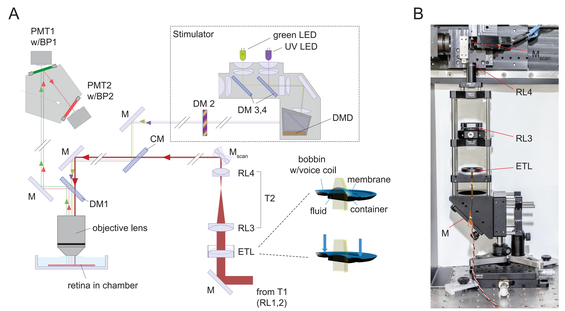

Figure 1 | Overview of 2P microscope equipped with mouse retina-specific visual stimulator and electrically tunable lens (ETL).
For simplicity, most lenses and silver mirrors (M) were omitted. **A**, A schematic diagram of excitation / detection pathway of 2P microscope. Dashed box: stimulus pathway, where grey area represents the "light engine" of DLP LightCrafter 4500 (Texas Instruments, Dallas, TX, USA), adapted for green/UV projection (by EKB Technologies Ltd, Israel). Inset: cross section and working principle of ETL-16-40-TC (Optotune, Switzerland). **B**, Photography of partial setup where ETL is installed (laser safety shielding removed). Cold mirror (CM), dichroic mirror (DM), band pass filter (BP), GaAsP photomultiplier tube (PMT), x-y galvo scanner (Mscan), relay lens (RL), telescope (T). (A), adapted from [1] & [Euler, Franke, Baden "Studying a light sensor with light: multiphoton imaging in the retina", in press]; (A) inset from [2].

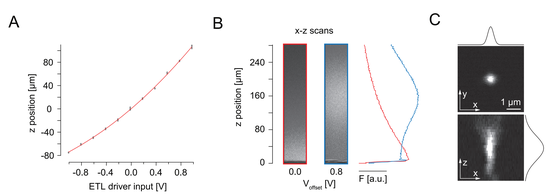

Figure 2 | Performance of axial scanning.
A, Steady state axial (z) position as a function of voltage input to ETL driver; each measurement (grey dots) was done in random sequence of input voltage (n=5); the red line is sigmoidal fit of mean values. **B**, Axial scans in sulforhodamine 101 (SR101) solution showing change in fluorescence intensity along the vertical axis for two different voltage offsets. Left: scan fields (x-z scan w/256x256 pixels @ 2ms/line; zoom xy, z=1.0, 0.8). Right: Axial fluorescence intensity distribution. **C**, Example of point spread function (PSF) in the x-y plane and along z-axis (measured with 170 nm beads, λ_{Peak}=515 nm). PSF-xy: 0.39-0.53 µm; PSF-z: 2.09-2.17 µm.

Functional Layering In The IPL

Light stimulus-evoked glutamate release across the IPL were recorded using iGluSnFR [4] unbiquitously expressed via AAV transduction (AAV2.hSynapsin.iGluSnFR or AAV2.7m8.hSynapsin.iGluSnFR; for AAV2.7m8 modification, see [5]). Bipolar cells exhibit functional layering across the IPL [6].

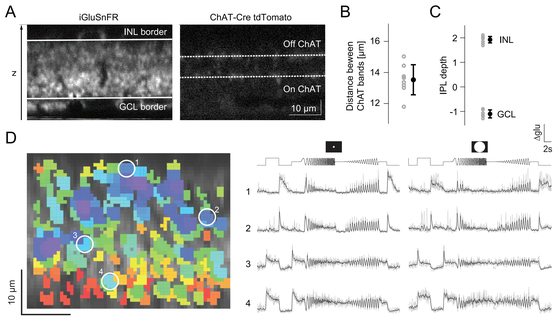

Figure 3 | Glutamate imaging in the IPL.
A, Axial scan of a whole-mount retina. Left: AAV-transduced iGluSnFR expression; right: tdTomato expression under the control of the ChAT promotor (x-z scan w/256x160 pixels @ 2ms/line). IPL borders and ChAT bands were defined manually. **B**, Distance between ChAT bands (13.52 ± 0.99 µm). **C**, Relative positions of IPL borders according to ChAT bands (INL: 1.92 ± 0.13; GCL: -1.09 ± 0.13). **D**, Examplary ROIs (left) and their responses (as change in glutamate release, Δglu) to a local (center) and a global (right) chirp light stimulus.
Panel B & C: from n=1/2/10 mouse/retinas/scans.

Batch Effects

Batch effects are variations in observed signals which arise from experimental factors, including temperature, fluorophore concentration, and the age or health of a particular retina. The magnitude of these effects can be large enough to obscure meaningful differences between bipolar cell types, making signal classification difficult.

Qualitatively, PCA plots suggest that the order of contributed variance is often:

On/Off split > Batch variability > Cell types

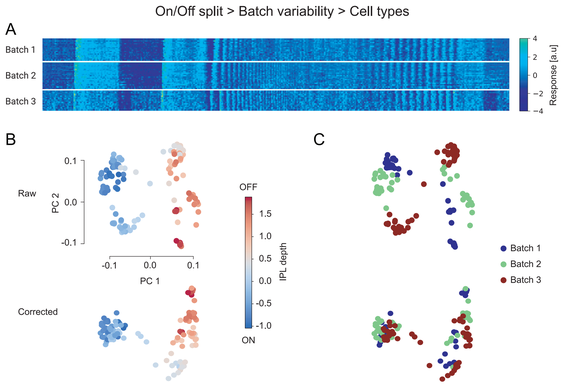

Figure 4 | Batch effects in axial scan recordings.
A, Traces from ON-layers of IPL in three axial scan recordings in response to local chirp stimulus. **B**, First two PCA components of local chirp responses, coloured by IPL depth, before and after linear batch correction. **C**, First two PCA components of local chirp responses, coloured by recording, before and after batch correction.

Linear Model of Batch Effects

Our initial approach was to use a linear fixed effects model to estimate the batch effect:

$$y = x_{Depth} + x_{Batch} * x_{On/Off} + \epsilon$$

where $x_{On/Off} \subset x_{Depth}$ and we set $x_{Batch} * x_{On/Off} \perp x_{Depth}$.

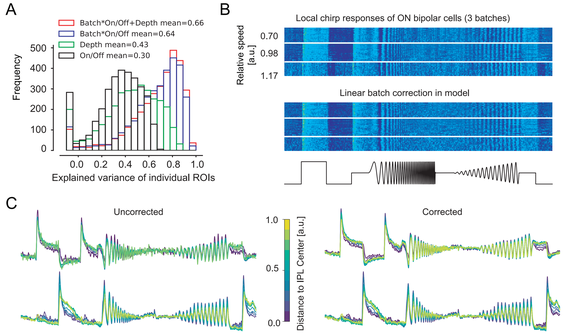

Figure 5 | Batch Effect Correction Using Linear Models.
A, Estimated r^2 for effects of ON-OFF, batch and depth in a linear model fitted to the local chirp response data. **B**, Response of IPL ON-layers in three recordings to local chirp stimulus, before and after linear batch correction. **C**, Linear model predictions for IPL responses at varying depths to local chirp stimulus, with and without batch effect correction.

Response Kinetics Hypothesis

Next, we tried to explore the nature of the batch corrections. Visual inspection of Fig. 4a suggests that batches have different response kinetics. This could be due to fluctuations of the temperature of the tissue and has also been suggested recently by [7]. To assess this, we computed the event-triggered-average temporal kernels and plotted the mean temporal kernel for each batch, finding that in the corrected data these become aligned (Fig 6a).

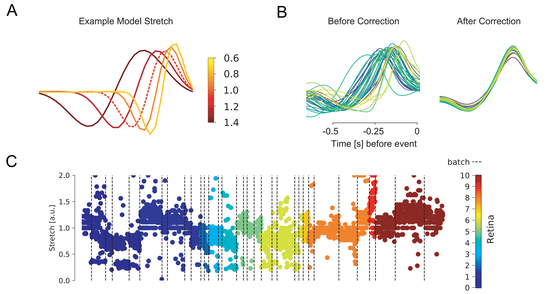

Figure 6 | Temporal Kinetics After Batch Effect Correction.
A, Mean event-triggered-average temporal kernels for each batch, before and after linear correction. **B**, Example kernels for model of "stretch" effect, for varying stretch parameters. **C**, Estimated stretch for each ROI, coloured by retina. One way ANOVA of retina effect on response speed: F ≈ 168.86, p < 10^{-8}.

Funding & Acknowledgements

This work was supported by the German Research Foundation (DFG) through Collaborative Research Center (CRC 1233) "Robust Vision" and DFG grants EC 479/1-1 and BE5601/4-1; the European Union's Horizon 2020 research and innovation programme under the Marie Skłodowska-Curie grant agreement No 674901; the German Excellency Initiative (EXC 307; EXC 2064); and the German Ministry of Research and Education through the Bernstein Award (01GQ1601). The research was also supported by Intelligence Advanced Research Projects Activity (IARPA) via Department of Interior/Interior Business Center (DoI/IBC) contract number D16PC00003. The U.S. Government is authorized to reproduce and distribute reprints for Governmental purposes notwithstanding any copyright annotation thereon. Disclaimer: The views and conclusions contained herein are those of the authors and should not be interpreted as necessarily representing the official policies or endorsements, either expressed or implied, of IARPA, DoI/IBC, or the U.S. Government. Neither do the authors endorse the views of the US government. We thank Deniz Dalkara (Institut de la Vision) for providing AAV2.7m8 and Dario Protti for discussion.

Temporal Alignment

We then incorporated the batch correction into a linear neural encoding model, where the temporal kernel was scaled by a batch-specific parameter α:

$$w = \sum_i \beta_i \sin \alpha t + \gamma_i \cos \alpha t$$

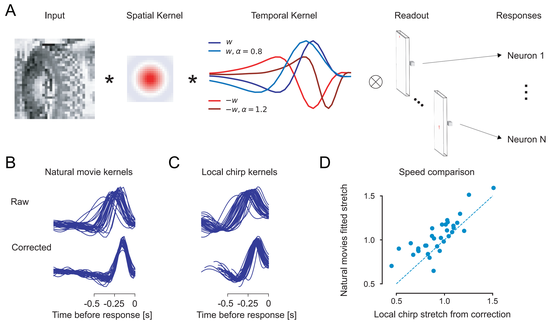

Figure 7 | Batch Effect Correction In A Linear Neural Encoding Model.
A, Schematic representaton of linear neural encoding model with batch correction (extending [7]). **B**, Temporal kernels learnt from encoding model fitted to IPL ON-layer responses to a natural movie stimulus. **C**, Temporal kernels learnt from encoding model, corresponding to the ROIs in B, fitted to responses to the local chirp stimulus. **D**, Estimated stretch factor for linear neural encoding models fitted to responses to natural movie stimulus and local chirp stimulus (Pearson's r: p = 0.82, p < 10^{-8}).

Functional Cell Types

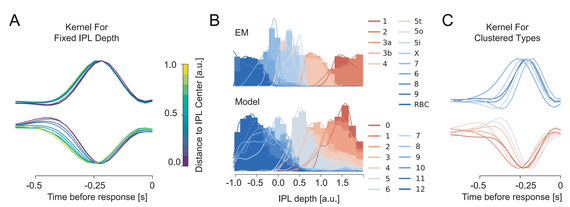

Figure 8 | Identification Of Functional Cell Types Following Batch Correction.
A, Estimated temporal kernels for ROIs at different IPL depths, assigned to depth-wise clusters. **B**, Stratification profiles of bipolar cell axon terminals for each type from a previously published electron microscopy dataset [9] (top). Estimated readout weights for temporal kernels from linear encoding model (bottom). **C**, Estimated temporal kernels from linear encoding model shown in B.

Conclusions

- The ETL allows the complete IPL to be scanned in a single recording
- When biological variation can be modelled and stimuli are identical, linear models can be deployed successfully to remove batch effects
- Where those conditions are untrue, a neural encoding model with a parametrised temporal kernel and a batch specific stretch allows cell types to be grouped across batches

References

[1] Euler et al. (2009) Pflugers Arch. 10.1007/s00424-008-0603-5.
[2] optotune.com/images/products/Optotune 20EL-16-40-TC.pdf
[3] Grewe et al. (2011) Biomed Opt Express, 10.1364/BOE.2.002035
[4] Marvin et al. (2013) Nat Meth 10.1038/nmeth.2333.
[5] Dalkara et al. (2013) 10.1126/scitranslmed.3005708.
[6] Franke, Berens et al. (2017) Nature, 10.1038/nature21394.
[7] Rhoades et al. (2018) bioRxiv. https://doi.org/10.1101/496455.
[8] Klindt et al. (2017) NeurIPS 30 (pp. 3506-3516).
[9] Helmstaedter et al. (2017) Nature, 500.7461.

UNIVERSITÄTS KLINIKUM TÜBINGEN
Institute for Ophthalmic Research

CIN Werner Reichardt Centre for Integrative Neuroscience

bccn tübingen